Dalton Transactions

PAPER

View Article Online
View Journal | View Issue

Cite this: *Dalton Trans.*, 2014, **43**, 16713

Tri- and tetra-nuclear polypyridyl ruthenium(II) complexes as antimicrobial agents

Anil K. Gorle,[a] Marshall Feterl,[b,c] Jeffrey M. Warner,[b,c] Lynne Wallace,[a] F. Richard Keene*[c,d,e] and J. Grant Collins*[a]

A series of inert tri- and tetra-nuclear polypyridylruthenium(II) complexes that are linked by the bis[4(4′-methyl-2,2′-bipyridyl)]-1,*n*-alkane ligand ("bb$_n$" for n = 10, 12 and 16) have been synthesised and their potential as antimicrobial agents examined. Due to the modular nature of the synthesis of the oligonuclear complexes, it was possible to make both linear and non-linear tetranuclear ruthenium species. The minimum inhibitory concentrations (MIC) of the ruthenium(II) complexes were determined against four strains of bacteria – Gram positive *Staphylococcus aureus* (*S. aureus*) and methicillin-resistant *S. aureus* (MRSA), and Gram negative *Escherichia coli* (*E. coli*) and *Pseudomonas aeruginosa* (*P. aeruginosa*). In order to gain an understanding of the relative antimicrobial activities, the cellular uptake and water–octanol partition coefficients (log *P*) were determined for a selection of the ruthenium complexes. Although the trinuclear complexes were the most lipophilic based upon log *P* values and showed the greatest cellular uptake, the linear tetranuclear complexes were generally more active, with MIC values <1 μM against the Gram positive bacteria. Similarly, although the non-linear tetranuclear complexes were slightly more lipophilic and were taken up to a greater extent by the bacteria, they were consistently less active than their linear counterparts. Of particular note, the cellular accumulation of the oligonuclear ruthenium complexes was greater in the Gram negative strains compared to that in the Gram positive *S. aureus* and MRSA. The results demonstrate that the lower antimicrobial activity of polypyridylruthenium(II) complexes towards Gram negative bacteria, particularly *P. aeruginosa*, is not strongly correlated to the cellular accumulation but rather to a lower intrinsic ability to kill the Gram negative cells.

Received 15th July 2014,
Accepted 19th September 2014

DOI: 10.1039/c4dt02139h

www.rsc.org/dalton

Introduction

Infectious diseases remain a leading cause of death worldwide, and as there is also an increasing emergence of drug-resistant bacteria[1] it is clear that there is a need for new antimicrobial agents. Based upon the versatile nature of transition metal complexes and their recent success as anticancer agents,[2–4] there has been growing interest in their use as antimicrobial agents, and in particular ruthenium complexes have been widely examined.[5–10] Dwyer and his co-workers first reported the antimicrobial potential of mononuclear iron and ruthenium complexes containing polypyridyl ligands.[11,12] However, while these complexes exhibited excellent activity against drug-sensitive strains, they were significantly less active against current drug-resistant strains.[13] In an attempt to increase the activity of inert polypyridylruthenium complexes against drug-resistant bacteria, we have examined the antimicrobial properties of inert and chlorido-containing dinuclear ruthenium and iridium metal analogues.[13–15] The inert dinuclear polypyridylruthenium(II) complexes $[\{Ru(phen)_2\}_2\{\mu\text{-bb}_n\}]^{4+}$ {"Rubb$_n$"; where phen = 1,10-phenanthroline; bb$_n$ = bis[4(4′-methyl-2,2′-bipyridyl)]-1,*n*-alkane for n = 5, 7, 10, 12 and 16} showed excellent activity, with minimum inhibitory concentrations (MIC) of 1 and 2 μg mL^{-1} for the Rubb$_{12}$ and Rubb$_{16}$ complexes against a range of Gram positive and Gram negative bacterial strains, and they maintained the activity against drug-resistant strains such as methicillin-resistant *Staphylococcus aureus* (denoted as MRSA).[13] Furthermore, preliminary toxicity assays against human red blood cells and a human monocytic leukemia cell line (THP-1) indicated that the Rubb$_n$ complexes were not significantly toxic to human cells.[13]

The inert dinuclear Rubb$_n$ complexes with an overall charge of 4+ can interact reversibly with various intra-cellular recep-

[a]*School of Physical, Environmental and Mathematical Sciences, University of New South Wales, Australian Defence Force Academy, Canberra, ACT 2600, Australia. E-mail: g.collins@adfa.edu.au*
[b]*School of Veterinary and Biomedical Sciences, James Cook University, Townsville, QLD 4811, Australia*
[c]*Centre for Biodiscovery and Molecular Development of Therapeutics, James Cook University, Townsville, QLD 4811, Australia*
[d]*School of Pharmacy and Molecular Sciences, James Cook University, Townsville, QLD 4811, Australia*
[e]*School of Chemistry and Physics, University of Adelaide, Adelaide, SA 5005, Australia. E-mail: richard.keene@adelaide.edu.au*

tors such as proteins and nucleic acids to stop bacterial cell replication. $Rubb_{16}$ was shown to condense ribosomes when they existed as polysomes, and it was postulated that the condensation of polysomes would halt protein production and thereby inhibit bacterial growth.[16] Although it would be expected that complexes which have a higher positive charge would condense polysomes more efficiently, cellular uptake experiments with mononuclear and dinuclear polypyridyliridium(III) complexes (3+ and 6+ respectively) demonstrated that they could not easily cross the cellular membrane, and hence they showed no antimicrobial activity.[15,17] An alternative approach of increasing the charge of the dinuclear ruthenium complexes is to synthesise tri- and tetra-nuclear species. While the tri- and tetra-nuclear ruthenium complexes will be more positively charged – 6+ and 8+ respectively – they will also be more lipophilic than the dinuclear counterparts due to the additional non-polar linking ligands. Preliminary experiments with the tri- and tetra-nuclear complexes of $Rubb_7$ demonstrated the potential of this approach.[13] The $Rubb_7$-tri and $Rubb_7$-tetra were 2–4 times more active against a range of bacteria than the corresponding dinuclear $Rubb_7$.

Over the last decade there has been considerable interest in developing inert dinuclear ruthenium(II) complexes as nucleic acid binding probes, anticancer agents and cellular imaging agents.[18–27] More recently, there has been increasing interest in using higher nuclearity ruthenium complexes as anticancer agents.[28–30] Predominantly, research has focused on ruthenium clusters or cages, as these bulky complexes may preferentially accumulate in tumours due to the enhanced permeability and retention effect.[28–30] Alternatively, while several tri- and tetra-nuclear copper(II) complexes with modest antimicrobial activities have been reported,[31,32] there have been very few studies on the potential of tri- or tetra-nuclear ruthenium complexes as antimicrobial agents. In the present study, we aimed to synthesise the tri- and tetra-nuclear analogues of the most active dinuclear complexes, $Rubb_{12}$ and $Rubb_{16}$, and examine their antimicrobial activities, log *P* values and cellular uptake. Additionally, due to the modular nature of the synthesis of these complexes, it was possible to synthesise both linear and non-linear tetranuclear complexes. The structures of the multinuclear complexes and the important precursor complex $Rubb_n$-Cl_2, which was also examined for antimicrobial activity, are shown in Fig. 1. The results of this study indicate that inert tri- and tetra-nuclear ruthenium polypyridyl complexes can be highly active antimicrobial agents.

Results

Synthesis

The synthesis of flexibly-linked dinuclear ($Rubb_n$-Cl_2), trinuclear ($Rubb_n$-tri), tetranuclear ($Rubb_n$-tetra) and non-linear tetranuclear ($Rubb_n$-tetra-nl) ruthenium complexes incorporating bis[4′-(4-methyl-2,2′-bipyridyl)]-1,*n*-alkane bridging ligands (bb_n) has been achieved in good yield, as shown in Schemes 1 and 2. The chlorido-containing dinuclear species ($Rubb_n$-Cl_2) were synthesised by reacting the mononuclear complex, $Rubb_n$-mono, with $(phenH^+)[Ru(phen)Cl_4]$ in DMF at reflux temperature. The characterisation of the chlorido complexes was carried out by NMR spectroscopy and they were used as precursors for the synthesis of the tri- and tetra-nuclear complexes.

The trinuclear and tetranuclear (both linear and non-linear) complexes were characterised by microanalysis, NMR (^1H and ^{13}C) and high resolution electrospray ionisation mass spectroscopy methods. Consistent with the observations previously reported for $Rubb_7$-tetra,[33] satisfactory ESI-MS could not be obtained for the linear tetranuclear complexes when they were dissolved in acetonitrile. However, good mass spectra could be obtained using acetone as the solvent. The synthesis of non-linear complexes was achieved by the reaction between the mononuclear complex, $Rubb_n$-mono, and *cis*-$[Ru(DMSO)_4Cl_2]$. The reaction was carried out in ethanol–water at reflux temperatures for 5–6 hours, whereupon all the DMSO and chlorido ligands were replaced by the free '2,2′-bpy' entities of $Rubb_n$-mono complexes. All the inert complexes (tri, tetra, tetra-nl species) were purified by cation exchange on an SP Sephadex C-25 column, whereas the chlorido-containing complexes ($Rubb_n$-Cl_2) were purified by size exclusion on an Sephadex LH-20 column.

It is noted that geometric isomers will exist for the oligonuclear complexes in this study. In the bridging ligands bb_n, the 2,2′-bipyridine coordinating moieties are unsymmetrically substituted – one pyridine entity with a methyl group in the 4-position and the other with the bridging methylene chain. Accordingly, for cases where there are two bb_n ligands attached to one metal centre – as is the case for the central ruthenium in the trinuclear complexes and the two central ruthenium centres in the linear tetranuclear species – the chain-bearing pyridine entities may bear either relative '*trans*' or one of two possible '*cis*' orientations (one symmetrical in the sense that the centre will have C_2 point group symmetry – denoted s-*cis* – and the other has C_1 point group symmetry – denoted u-*cis*). For the trinuclear case ($Rubb_n$-tri) there are three isomers possible based on the central metal centre (*trans*, s-*cis* and u-*cis*), and six isomers based on the two internal metal centres (*trans*, *trans*; s-*cis*,s-*cis*; u-*cis*,u-*cis*; *trans*,s-*cis*; *trans*,u-*cis*; s-*cis*,u-*cis*) for the linear tetranuclear case ($Rubb_n$-tetra). For the dinuclear $Rubb_n$-Cl_2 complexes the two chlorido ligands may bear either a *cis*,*cis* or a *cis*,*trans* relationship to the chain-bearing pyridine entity, so that there are two isomers. Finally, in the case of the non-linear tetranuclear complexes, $Rubb_n$-tetra-nl, the central Ru centre has three bb_n ligands attached so that the chain-bearing pyridine entities may bear either a facial or meridional orientation to one another – giving rise to two isomers (*fac* and *mer*). In the case of *fac*/*mer* geometric isomerism, the *mer* isomer is thermodynamically preferred for statistical reasons (3/1) but the *mer*/*fac* ratio is often considerably greater than that because of steric congestion in the *fac* form.[34] In the present case for the tetra-nl species, 2D NMR studies (COSY and ROESY – not reported) indicated the existence of both isomers with the *fac* isomer comprising about 5% (*mer*/*fac* =

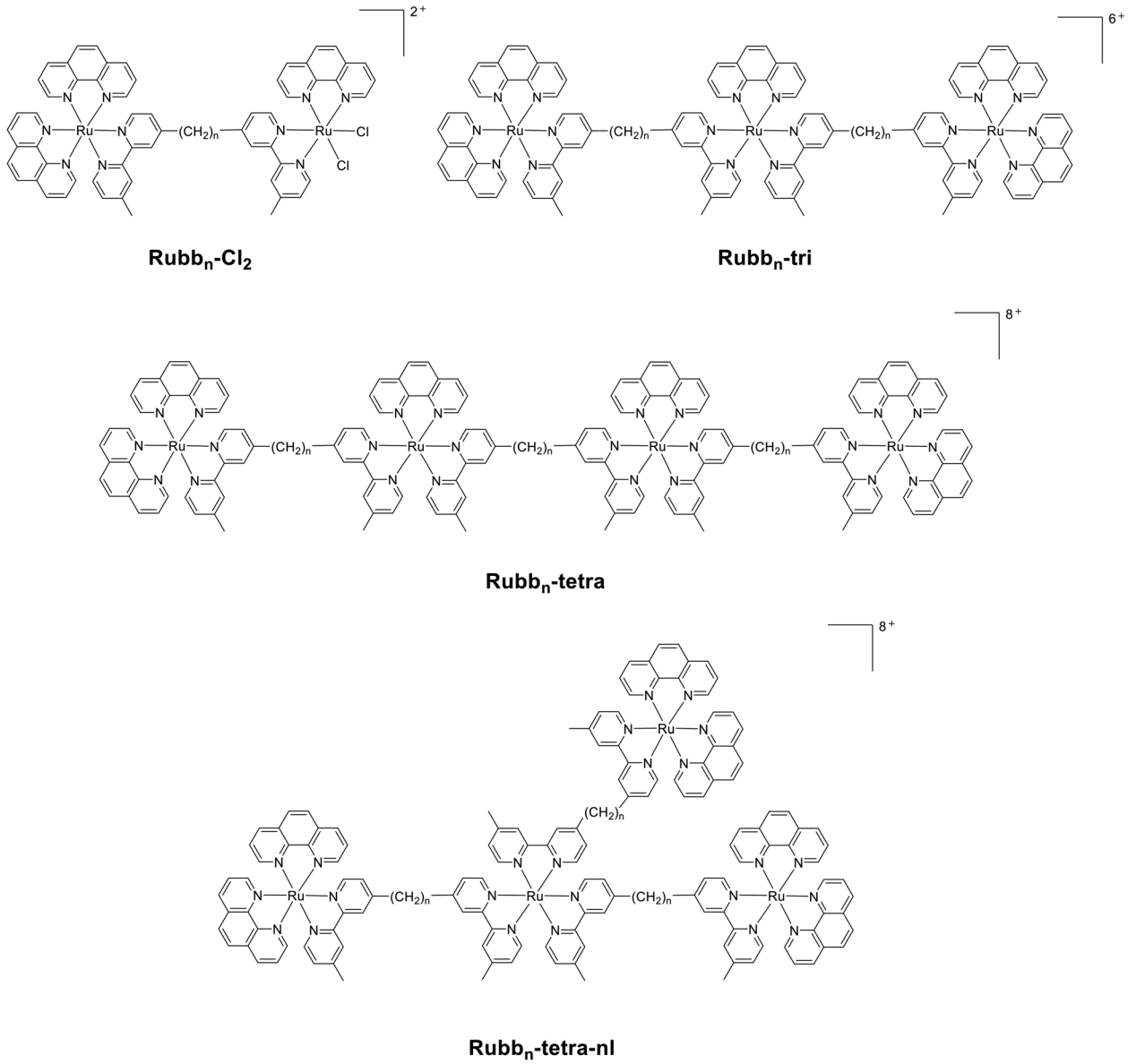

Fig. 1 Chlorido-containing dinuclear complexes (Rubb$_n$-Cl$_2$); and the inert trinuclear (Rubb$_n$-tri) and tetranuclear (linear Rubb$_n$-tetra, and non-linear Rubb$_n$-tetra-nl) ruthenium(II) complexes.

19/1). The separation of possible geometrical isomers was not attempted for any of the complex systems in this study at this stage, and would represent a significant challenge in a number of these cases.

In agreement with previous studies, the Rubb$_n$-Cl$_2$ complexes hydrolysed when they were dissolved in water.[35,36] The aromatic region of the ^{1}H NMR spectrum of a Rubb$_n$-Cl$_2$ complex dissolved in water was extremely complicated suggesting a mixture of $[\text{Rubb}_n(\text{OH}_2)\text{Cl}]^+$ and $[\text{Rubb}_n(\text{OH}_2)_2]^{2+}$ species, as has been previously observed for the hydrolysis of *cis*-$[\text{Ru(bpy)}_2\text{Cl}_2]$.[36] Consistent with this proposal, the addition of $AgNO_3$ to a Rubb$_n$-Cl$_2$ complex that had been in an aqueous solution for two days did induce some changes in the NMR spectrum. However, even after the addition of $AgNO_3$, the aromatic region in the NMR spectrum was still very complex. This could indicate that both the *cis*- and *trans*-diaqua species were formed, as has been noted in the acid hydrolysis of $[\text{Ru(CO}_3)\text{(bpy)}_2]$.[37]

Electrochemistry

Cyclic voltammetry was used to determine the redox potentials for the multinuclear complexes with n = 12 (Table 1). All complexes showed a single, reversible Ru(II/III) oxidation peak at ≈+1.27 V *vs.* Ag/AgCl, and a series of ligand-based reductions, consistent with the well-established behaviour of tris(bidentate) polypyridylruthenium complexes.[38,39] It was thought that differences might be discernible in the potentials, particularly the reduction patterns, given the subtle structural variations in the different metal centres in the multinuclear complexes. For example it has been established that in the homoleptic

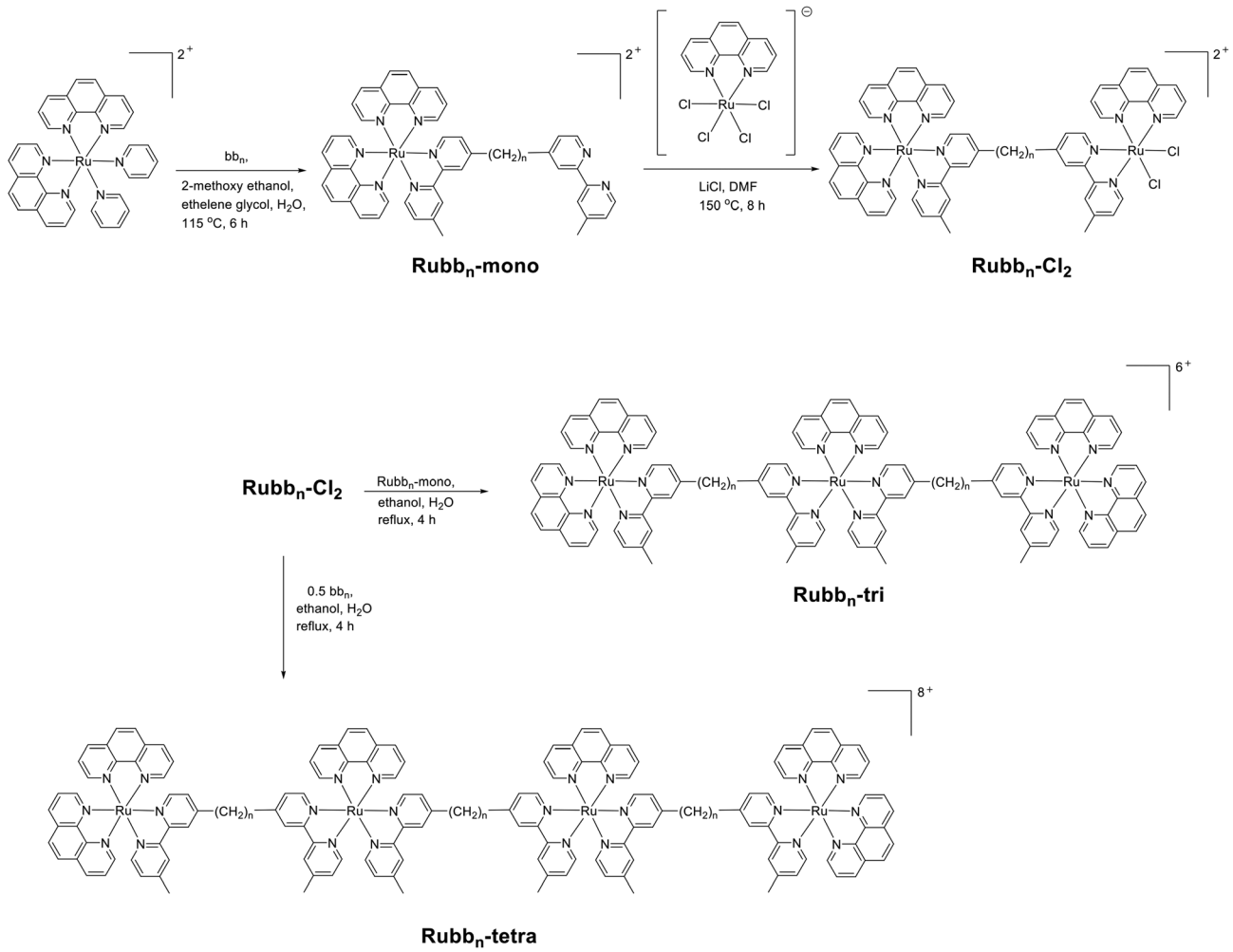

Scheme 1

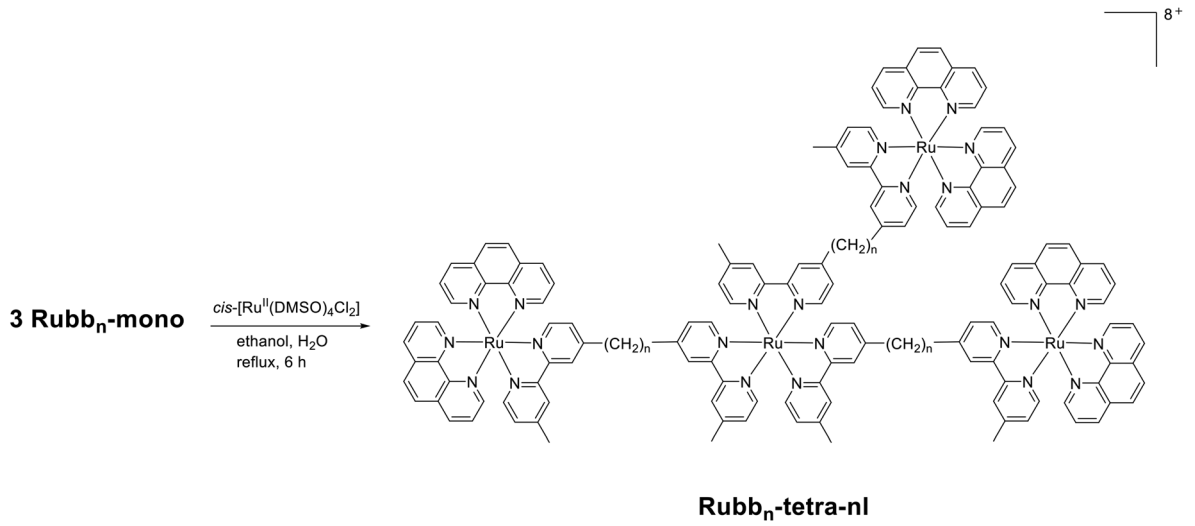

Scheme 2

Table 1 Electrode potentials for Ru(II) complexes in CH_3CN (in V *vs.* Ag/AgCl)

Complex	Oxidation $\{E_{1/2}$ Ru(II/III)$\}$	Reductions $(E_{pc})^a$
$Rubb_{12}$	1.26	−1.33, −1.52, −1.92
$Rubb_{12}$-tri	1.28	−1.32, −1.49, −1.85[b]
$Rubb_{12}$-tetra	1.26	−1.33, −1.50, −1.84[b]
$Rubb_{12}$-tetra-nl	1.27	−1.32, −1.49, −1.85[b]

[a] Irreversible/semi-reversible; cathodic peak given. [b] Weak.

complexes $[Ru(phen)_3]^{2+}$ and $[Ru(Me_2bpy)_3]^{2+}$, the Me_2bpy ligand is slightly more difficult to reduce than phen due to the electron-donating effect of the methyl groups, and this also translates to an effect on the Ru(II) centre, which undergoes oxidation more readily.[39,40] Either terminal of the bb_{12} ligand could be expected to mimic a Me_2bpy ligand, as has been observed for the complex $[\{(bpy)_2Ru\}_2(bb_2)]^{4+}$, which shows very similar redox potentials to the mononuclear complex $[Ru(bpy)_2(Me_2bpy)]^{2+}$.[41] In the present case, no significant differences were observed in the oxidation potentials of the complexes, even for the non-linear tetranuclear complex, in which the central ruthenium differs somewhat more from the others. The reduction patterns were also quite similar, with each complex showing two closely-spaced reductions. A third clear reduction peak was observed for $Rubb_{12}$, though this was distorted by adsorption. This three-reduction set is consistent with the pattern reported for both mononuclear $[Ru(L)_2(Me_2bpy)]^{2+}$ (L = bpy, phen) and dinuclear $[\{Ru(bpy)_2\}_2\}(bb_n)]^{4+}$ (n = 2,3).[41–43] For the tri- and tetra-nuclear complexes only a small peak was evident at potentials where a third reduction might be expected, and a desorption peak was generally observed in the re-oxidation scan. Adsorption of reduction products has previously been noted for other multinuclear ruthenium bipyridyl complexes.[44,45] The results indicate that redox differences between the complexes are negligible and unlikely to underpin any differences in biological activity.

Antimicrobial activity

The minimum inhibitory concentrations (MIC) for the di-, tri- and tetra-nuclear ruthenium complexes against four bacterial strains {*Staphylococcus aureus* (*S. aureus*), methicillin-resistant *S. aureus* (MRSA), *Escherichia coli* (*E. coli*) and *Pseudomonas aeruginosa* (*P. aeruginosa*)} have been determined and the results are summarised in Table 2. The results demonstrate that some of the ruthenium(II) complexes in the present study have significant antimicrobial activity against both classes of bacteria, and most of the complexes are more active against Gram positive bacteria than the Gram negative strains. Of particular note, the inert tri- and tetra-nuclear ruthenium complexes showed better antimicrobial activity than the corresponding dinuclear ruthenium(II) complexes ($Rubb_n$), particularly when the MIC values are given on a molar basis. Interestingly, the non-linear tetranuclear ruthenium(II) complexes ($Rubb_n$-tetra-nl) were two-fold less active than the dinuclear $Rubb_n$ complexes. Of all the complexes, $Rubb_{12}$-tri, $Rubb_{16}$-tri, $Rubb_{12}$-tetra and $Rubb_{16}$-tetra are the most active compounds, and are up to four-times more active than the dinuclear counterparts against Gram positive and slightly more active against the Gram negative strains. Furthermore, $Rubb_{12}$-tri, $Rubb_{16}$-tri, $Rubb_{12}$-tetra and $Rubb_{16}$-tetra are 4–8 times more active than the previously reported $Rubb_7$-tri and $Rubb_7$-tetra complexes.[13] Even though the overall charge of the linear and non-linear version of the tetranuclear complexes is the same (8+), the non-linear tetranuclear ruthenium complexes ($Rubb_n$-tetra-nl) are less active when compared to the corresponding linear species, suggesting that the linearity could play an important role in inhibiting bacterial growth. The dinuclear ruthenium(II) complexes with two chlorido ligands ($Rubb_n$-Cl_2) also showed good activity, but are fractionally less active than the tri- and tetra-nuclear complexes. In general, complexes with the bb_{12} linking ligand were the most active against *S. aureus*, MRSA, and *E. coli*, with the complexes having the shortest (bb_{10}) and longest (bb_{16}) linking chain being the least active. However, against *P. aeruginosa*, complexes with the bb_{16} linking ligand showed better activity.

Table 2 MIC values (μM) for the ruthenium complexes after 16–18 hours of incubation against Gram positive and Gram negative bacterial strains

	Gram positive		Gram negative	
Compounds	*S. aureus*	MRSA	*E. coli*	*P. aeruginosa*
$Rubb_{12}$	0.6	0.6	2.5	20.1
$Rubb_{16}$	1.2	1.2	2.4	9.8
$Rubb_{10}$-tri	0.8	1.7	1.7	13.5
$Rubb_{12}$-tri	0.4	0.8	1.6	13.1
$Rubb_{16}$-tri	0.4	0.8	3.1	12.6
$Rubb_{10}$-tetra	1.2	2.5	2.5	19.9
$Rubb_{12}$-tetra	0.3	0.6	1.2	9.7
$Rubb_{16}$-tetra	0.3	0.6	2.3	9.2
$Rubb_{10}$-tetra-nl	2.5	2.5	5.0	19.9
$Rubb_{12}$-tetra-nl	1.2	1.2	4.9	19.4
$Rubb_{16}$-tetra-nl	1.1	2.3	4.6	18.5
$Rubb_{10}$-Cl_2	5.9	5.9	5.9	46.9
$Rubb_{12}$-Cl_2	1.4	1.4	2.9	23.0
$Rubb_{16}$-Cl_2	1.4	2.8	5.5	44.2
Ampicillin	<0.7	183.0	11.4	> 366.0
Gentamicin	<0.5	66.9	1.0	0.5

Due to their greater lipophilicity (see below), it was considered that the antimicrobial activity of the tri- and tetranuclear complexes could decrease to a greater extent with longer incubation times than would the dinuclear complexes. Table 3 summarises the MIC values for the ruthenium complexes when the assays were carried out over a 20–22 hour timeframe. The MIC values for the tri- and tetra-nuclear complexes increased by as much as four-fold for some of the complexes when compared to the 16–18 hour values. Alternatively, the dinuclear complexes $Rubb_{12}$ and $Rubb_{16}$ only exhibited a maximum two-fold decrease in activity across the four bacteria. These observations suggest that the tri- and tetra-nuclear complexes rapidly accumulate within the bacteria, thereby decreasing the concentration in the incubation broth. However, even

Table 3 MIC values (μM) for the ruthenium complexes after 20–22 hours of incubation against Gram positive and Gram negative bacterial strains

	Gram positive		Gram negative	
Compound	*S. aureus*	MRSA	*E. coli*	*P. aeruginosa*
$Rubb_{12}$	1.3	2.5	5.0	40.3
$Rubb_{16}$	1.2	2.4	4.9	19.6
$Rubb_{10}$-tri	1.7	3.4	3.4	27.0
$Rubb_{12}$-tri	1.6	1.6	3.3	26.3
$Rubb_{16}$-tri	1.6	1.6	6.3	25.1
$Rubb_{10}$-tetra	2.5	5.0	5.0	19.9
$Rubb_{12}$-tetra	0.6	1.2	2.4	9.7
$Rubb_{16}$-tetra	1.1	1.1	2.3	9.2
$Rubb_{10}$-tetra-nl	5.0	5.0	9.9	19.9
$Rubb_{12}$-tetra-nl	1.2	2.4	4.9	19.4
$Rubb_{16}$-tetra-nl	2.3	2.3	4.6	18.5
$Rubb_{10}$-Cl_2	5.9	11.7	5.9	46.9
$Rubb_{12}$-Cl_2	2.9	1.4	5.7	23.0
$Rubb_{16}$-Cl_2	2.8	2.8	11.0	44.2
Ampicillin	<0.7	183.0	11.4	>366.0
Gentamicin	<0.5	66.9	1.0	0.5

at the longer incubation time $Rubb_{12}$-tetra and $Rubb_{16}$-tetra are the most active of all the ruthenium complexes tested.

The minimum bactericidal concentrations (MBC) of a selection of the ruthenium complexes were determined after the MIC values were obtained for the 20–22 hour incubation experiment. The results are summarised in Table 4. As the MBC values are generally ≤2 × MIC for the 20–22 hour incubation, it can be concluded that the tri- and tetra-nuclear complexes are bactericidal rather than bacteriostatic.

Log *P*

Lipophilicity is a significant factor that affects the biological activity of any metal complex, as it is generally correlated to the capacity of the drug to penetrate through the cell membrane. The standard octanol-water partition coefficient (log *P*) was determined for the mononuclear species $[Ru(phen)_2(Me_2bpy)]^{2+}$ and $Rubb_n$ (as control experiments), $Rubb_n$-tri, $Rubb_n$-tetra and $Rubb_n$-tetra-nl complexes, and the results are summarised in Table 5. From the results, the trinuclear ruthenium complexes are more lipophilic than the tetranuclear ruthenium complexes. For the dinuclear $Rubb_n$ complexes, the antimicrobial activity was directly related to the log *P*, with activity increasing with increasing lipophilicity. However, although the trinuclear complexes were more lipophilic than their corresponding linear tetranuclear complexes, they were less active. This suggests lipophilicity is an important determinant of activity, but only to the level that allows the ruthenium complex to easily diffuse across the cellular membrane.

Table 4 MBC values (μM) for a selection of the ruthenium complexes against Gram positive and Gram negative bacterial strains

	Gram positive		Gram negative	
Compound	*S. aureus*	MRSA	*E. coli*	*P. aeruginosa*
$Rubb_{12}$	2.6	2.5	10.1	40.3
$Rubb_{12}$-tri	3.3	3.3	6.6	52.6
$Rubb_{16}$-tri	1.6	6.3	12.6	50.3
$Rubb_{12}$-tetra	1.2	1.2	2.4	19.4
$Rubb_{16}$-tetra	2.3	2.3	4.6	37.0

Table 5 Octanol–water partition coefficients (log *P*) for the ruthenium complexes

Metal complex	Charge	log *P*
$[Ru(phen)_2(Me_2bpy)]^{2+}$	+2	−2.9
$Rubb_{12}$	+4	−2.9
$Rubb_{16}$	+4	−1.9
$Rubb_{10}$-tri	+6	−1.3
$Rubb_{12}$-tri	+6	−1.0
$Rubb_{16}$-tri	+6	−0.8
$Rubb_{10}$-tetra	+8	−1.7
$Rubb_{12}$-tetra	+8	−1.6
$Rubb_{16}$-tetra	+8	-0.9_5
$Rubb_{10}$-tetra-nl	+8	−1.9
$Rubb_{12}$-tetra-nl	+8	−1.4
$Rubb_{16}$-tetra-nl	+8	−1.1

Cellular accumulation

The cellular accumulations of the tri- and tetra-nuclear ruthenium complexes in *S. aureus*, MRSA, *E. coli*, and *P. aeruginosa* were determined by measuring the concentration of the complex remaining in the culture supernatant after removing the bacteria by centrifugation. The concentration of the ruthenium complex in the supernatant was calculated from an absorbance calibration curve obtained by adding known concentrations of the ruthenium complex to a blank supernatant. As the absorbance of the ruthenium complexes varied with the different broths and supernatants for each bacterial strain, a calibration curve was determined for each complex in the supernatant of each bacterial strain. The uptake of complexes into bacterial strains was measured at various incubation time points, however the uptake did not significantly change with incubation time after 30 minutes. Fig. 2 shows the uptake of the ruthenium complexes into the bacteria after 30 minutes. Surprisingly, the uptake of the complexes is slightly higher for the Gram negative bacteria than the Gram positive. The

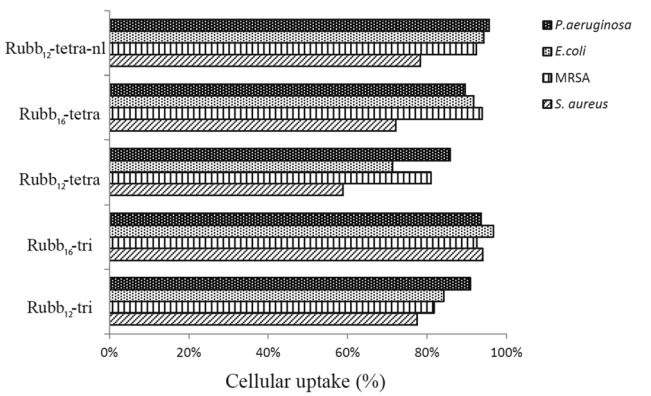

Fig. 2 Cellular uptake of the ruthenium complexes into four bacteria after a 30 minute incubation.

accumulation of $Rubb_{16}$-tri was the highest in both Gram positive and Gram negative bacteria. For all the complexes lower levels of accumulation were observed for *S. aureus*, compared to the other bacteria. For both the Gram positive and Gram negative bacteria, the cellular accumulation of the tetranuclear metal complexes was slightly lower than with the trinuclear counterparts. Surprisingly, the uptake of $Rubb_{12}$-tetra-nl is greater than $Rubb_{12}$-tetra and $Rubb_{12}$-tri.

Discussion

We have previously shown that dinuclear ruthenium(II) complexes ($Rubb_n$) exhibit excellent antimicrobial properties in terms of MIC values, cellular uptake, time-kill curves and show low toxicity towards human cells.[13] In order to further improve the antimicrobial properties, we have synthesised the tri- and tetra-nuclear ruthenium(II) analogues of the most active dinuclear complexes, $Rubb_{12}$ and $Rubb_{16}$, and examined their *in vitro* susceptibility, lipophilicity and cellular accumulation. The results of the MIC assays indicate that the linear tetranuclear complexes, $Rubb_n$-tetra, are consistently more active across the four bacteria used in this study than $Rubb_{12}$ and $Rubb_{16}$. Alternatively, the trinuclear analogues of $Rubb_{12}$ and $Rubb_{16}$ are slightly more active against some bacteria than the corresponding dinuclear complexes, but slightly less active in others. In a similar manner to $Rubb_{12}$ and $Rubb_{16}$, the tri- and tetra-nuclear linear complexes maintain their activity against MRSA compared to *S. aureus*, and are bactericidal. The non-linear tetranuclear complexes, $Rubb_n$-tetra-nl, are consistently less active than their linear counterparts and $Rubb_{12}$ and $Rubb_{16}$. Significantly, whereas $Rubb_{10}$-tri was generally more active than $Rubb_{10}$-tetra, the activity of $Rubb_n$-tetra was greater than $Rubb_n$-tri for n = 12 and 16 over the four bacterial strains used in the study.

The lipophilicity of the ruthenium complexes, as determined by log *P*, increased in the order $Rubb_n$ < $Rubb_n$-tetra < $Rubb_n$-tri, with all tri- and tetra-nuclear complexes being significantly more lipophilic than $Rubb_{16}$. As the ruthenium complexes enter bacterial cells by passive diffusion,[46] it is not surprising that the cellular accumulation experiments demonstrated that the tri- and tetra-nuclear complexes rapidly accumulate to high concentrations within the bacteria. However, the extent of the cellular accumulation of the tri- and tetra-nuclear complexes in the Gram negative bacteria, particularly *P. aeruginosa*, is surprising. The results of this study demonstrate that the lower toxicity of the dinuclear complexes towards *P. aeruginosa* is probably not strongly correlated to the cellular accumulation – as we previously concluded – but rather to a lower intrinsic ability to kill *P. aeruginosa* cells. Preliminary pharmacokinetic experiments with mice have indicated that $Rubb_{12}$ and $Rubb_{16}$ are rapidly cleared from the blood;[47] consequently, the greater lipophilicity and greater cellular uptake may be advantageous for *in vivo* antimicrobial studies.

Interestingly, the one non-linear tetranuclear complex examined in cellular accumulation experiments, $Rubb_{12}$-tetra-nl, showed greater accumulation than the corresponding linear complex $Rubb_{12}$-tetra. Despite $Rubb_{12}$-tetra-nl being slightly more lipophilic than $Rubb_{12}$-tetra, it would be expected that the linear complex would cross a cell membrane more easily than a non-linear complex. However, as the ruthenium complexes enter bacterial cells by passive diffusion,[47] the level of the cellular accumulation is a function of the binding of the ruthenium complex to intra-cellular receptors, such as nucleic acids and proteins. Despite the relatively greater accumulation of $Rubb_{12}$-tetra-nl compared to $Rubb_{12}$-tetra, the linear complex exhibited greater activity. Previous studies have shown that because of the flexibility of the alkane chain in the bb_n ligand, both ruthenium metal centres in the $Rubb_n$ complexes can closely associate with the DNA minor groove.[48] Similarly, the linear tetranuclear complexes could also follow the curvature of the DNA groove allowing close association of the four ruthenium centres with the DNA backbone. Alternatively, due to the three-dimensional shape of the non-linear tetranuclear complexes, the interactions with DNA would be substantially different and a different biological response would be expected.

There has been increasing interest in trinuclear and higher nuclearity ruthenium complexes as anticancer agents.[28–30] However, there have been very few studies on the potential of tri- or tetra-nuclear ruthenium complexes as antimicrobial agents. The present study indicates that these multinuclear complexes are highly active antimicrobial agents. Consequently, using the $Rubb_n$ scaffold as a starting point, oligonuclear ruthenium complexes can be synthesised which vary by almost two orders of magnitude in lipophilicity, but contain a higher charge and remain water-soluble. Furthermore, the higher nuclearity complexes would be expected to display different nucleic acid binding or condensation potential and exhibit different pharmacokinetic profiles. Given the rapid uptake and high level of accumulation of the tetranuclear complexes in bacteria, it is unlikely that pentanuclear or higher nuclearity complexes would be more effective antimicrobial agents.

Experimental

Physical measurements

^{1}H NMR and ^{13}C NMR spectra were recorded on a Varian Advance 400 MHz spectrometer at room temperature in D_2O {99.9%, Cambridge Isotope Laboratories (CIL)}, $CDCl_3$ (99.8%, CIL), or CD_3CN (>99.8%, Aldrich), or CD_3OD (>99.8%, Aldrich). UV absorbance was measured on a Jenway 6300 spectrophotometer. Microanalyses were performed by the Microanalytical Unit, Research School of Chemistry, Australian National University, Canberra. High-resolution mass spectral measurements were made using a Waters LCT mass spectrometer (Research School of Chemistry, Australian National University).

Materials and methods

Tetraethylammonium chloride, 2-methoxyethanol, lithium chloride, potassium hexafluorophosphate (KPF_6) and ammonium hexafluorophosphate (NH_4PF_6) were purchased from Aldrich and used as supplied; Amberlite® IRA-402 (chloride form) anion-exchange resin, SP-Sephadex C-25 cation exchanger and Sephadex® LH-20 were obtained from GE Health Care Bioscience. Cation-adjusted Mueller-Hinton broth (CAMHB) was purchased from Fluka, Gillingham, UK; the control antibiotics gentamicin and ampicillin were purchased from Oxoid, Australia. The syntheses of ligands bb_n (n = 10, 12 and 16) and $[Ru(phen)_2(py)_2]Cl_2$, $(phenH^+)[Ru(phen)Cl_4]$, *cis*-$[Ru(DMSO)_4Cl_2]$ were performed according to reported literature methods.[33,49–51]

Bacterial strains

All bacterial strains are classified as C2 risk group and must be handled within a PC2 laboratory. Two *Staphylococcus aureus* (Gram positive) isolates, a methicillin-susceptible *S. aureus* strain (ATCC 25923), a clinical multidrug-resistant MRSA strain (a wild clinical strain from the JCU culture collection) and two Gram negative isolates *Escherichia coli* (ATCC 25922) and *Pseudomonas aeruginosa* (ATCC 27853) were used for *in vitro* antimicrobial studies.

MIC and MBC determination

The MIC tests were conducted by the broth micro-dilution method in duplicate as outlined in the CLSI guidelines.[52] The MBC tests were performed in duplicate according to the standard microbiological techniques protocol.[53] The bacteria were grown on Mueller-Hinton agar and suspended in growth medium CAMHB. Bacterial inocula were adjusted to a turbidity equivalent to that of a 0.5 McFarland standard and diluted to a final concentration of 4–8 × 10^5 cfu mL^{-1}. Compounds tested were dissolved and serially diluted in cation-adjusted Mueller–Hinton broth (CAMHB; Fluka, Gillingham, UK) in sterile 96-well flat-bottom plates to a final volume of 100 μL in each well. An equal volume of inocula was added to each well, making a final concentration range of the compounds tested, including the control antibiotics gentamicin and ampicillin (Oxoid, Australia), of between 0.25 and 128 mg L^{-1}. MICs were recorded after 16–18 h and 20–22 h of incubation at 37 °C. Colony counts of the inocula were performed for determination of the MBC. After MIC results were noted, the incubation was continued for another 4 h, the wells with no visible growth were taken into colony counting and the concentration of compounds that produced a 99.9% kill relative to the starting inoculum was recorded as the MBC.

Cellular uptake

The cellular uptake of the ruthenium complexes was measured by monitoring the UV absorbance of the complexes remaining in the supernatant of the cultures after incubation for various periods of time. Bacterial inocula in log phase were adjusted to a cell concentration from 1–5 × 10^7 cfu mL^{-1}. Aliquots (2 mL) of the adjusted inocula were placed in glass culture tubes and 50 μL of stock solution (330 mg L^{-1}) of the ruthenium complex was added to give a final concentration of 8 mg L^{-1}. Control flasks containing 50 mL of each bacterial suspension were set up as blank samples to obtain UV calibration curves for each complex. Culture tubes and control flasks were incubated with agitation at 150 rpm at 37 °C for 0.5, 1, 1.5 or 2 h. At the end of incubation, the culture tubes were centrifuged (*S. aureus* and MRSA at 6000*g*; *E. coli* and *P. aeruginosa* at 17 000*g*) at 4 °C for 10 min. Supernatants (1.6 mL) were carefully transferred to 2 mL tubes and the UV absorbance of the remaining ruthenium complex was measured at λ = 488 nm. Volumes (10, 30, 40, 50 and 65 μL) of a stock solution (330 mg L^{-1}) of each complex were added to 2 mL aliquots of the supernatant from each control bacterial suspension (untreated with drug) to acquire a UV-concentration linear correlation chart for calibration. The uptake of the complexes was calculated by using the calibration curve obtained from control bacterial aliquots.

Lipophilicity (log *P*) determination

The partition coefficients (log *P*) were measured using the shake-flask technique: each ruthenium complex (at 0.1 mM) was dissolved in the water phase and an equal volume of *n*-octanol was added. The two phases were mutually saturated by shaking overnight at ambient temperature and then were allowed to separate on standing. The concentration of the metal complex in each phase was determined spectrophotometrically at λ = 450 nm.

Electrochemistry

Cyclic voltammetry was carried out using an eDAQ EA161 potentiostat operated *via* an eDAQ ED401 e-corder. A glassy carbon working electrode, platinum wire counter electrode and Ag/AgCl reference electrode were used. Ferrocene was used as an internal reference check.[54] HPLC grade acetonitrile was used as solvent and the supporting electrolyte was 0.1 M tetra-*n*-butylammonium tetrafluoroborate.

Synthesis of metal complexes

$[Ru(phen)_2(bb_n)](PF_6)_2$ ($Rubb_n$-mono). The mononuclear ruthenium(II) complexes $Rubb_n$-mono were synthesised as previously described (n = 7 and 16),[33] with typical yields being 50–60%. The ^{1}H NMR spectrum of $Rubb_{16}$-mono was consistent with that previously reported.[33] **$[Ru(phen)_2(bb_{12})](PF_6)_2 \cdot 2H_2O$** Anal. Calcd for $C_{58}H_{62}N_8F_{12}O_2P_2Ru$: C, 53.8%; H, 4.83%; N, 8.7%. Found: C, 53.9%; H, 4.80%; N, 8.5%. ^{1}H NMR (400 MHz, CD_3CN): δ 8.63 (d, J = 8.0 Hz, 2H); 8.52 (dd, J = 8.2 Hz, 3.3 Hz, 2H); 8.40 (s, 2H); 8.35 (s, 2H); 8.26–8.17 (m, 8H); 7.88–7.85 (m, 2H); 7.78 (dd, J = 8.1 Hz, 5.1 Hz, 2H); 7.56–7.51 (m, 2H); 7.50–7.46 (m, 2H); 7.22–7.17 (m, 2H); 7.10 (t, J = 9.0 Hz, 2H); 2.76 (t, J = 7.6 Hz, 2H); 2.67 (t, J = 7.2 Hz, 2H); 2.51 (s, 3H); 2.41 (s, 3H); 1.70–1.56 (m, 4H); 1.35–1.17 (m, 16H). **$[Ru(phen)_2(bb_{10})](PF_6)_2 \cdot 3H_2O$** Anal. Calcd for $C_{56}H_{60}N_8F_{12}O_3P_2Ru$: C, 52.4%; H, 4.71%; N, 8.7%. Found: C, 52.2%; H, 4.47%; N, 8.5%. ^{1}H NMR (400 MHz, CD_3CN): δ 8.63

(d, J = 8.0 Hz, 2H); 8.48 (dd, J = 10.6 Hz, 4.7 Hz, 2H); 8.40 (s, 2H); 8.35 (s, 2H); 8.27–8.16 (m, 8H); 7.87 (d, J = 4.8 Hz, 2H); 7.81–7.75 (m, 2H); 7.57–7.51 (m, 2H); 7.48 (t, J = 6.4 Hz, 2H); 7.22–7.17 (m, 2H); 7.12–7.08 (m, 2H); 2.76 (t, J = 7.4 Hz, 2H); 2.68 (t, J = 7.5 Hz, 2H); 2.50 (s, 3H); 2.41 (s, 3H); 1.70–1.59 (m, 4H); 1.36–1.24 (m, 12H).

[{Ru(phen)$_2$}(μ-bb$_n$){Ru(phen)Cl$_2$}]Cl$_2$ (Rubb$_n$-Cl$_2$). [Ru(phen)$_2$-(bb$_{12}$)](PF$_6$)$_2$ (450 mg, 0.35 mmol), (phenH$^+$)[Ru(phen)Cl$_4$] (216 mg, 0.35 mmol) and lithium chloride (280 mg) were dissolved in dry DMF (28 mL) and the mixture was stirred at 150 °C for 8 h in the dark under a nitrogen atmosphere. After cooling the reaction mixture to room temperature, acetone (80 ml) was added and the product precipitated as a dark brown material, which was kept with the mother liquor in the fridge for 16 h. The precipitate was then filtered and washed with acetone (40 mL), dried under *vacuo* and redissolved in ethanol (20 mL). Solid NH_4PF_6 (200 mg) was added to the ethanol solution, resulting in the precipitation of the PF_6^- salt of the complex, which was then filtered and washed with ethanol (2 × 20 mL) and diethyl ether (2 × 20 mL) to afford a dark brown solid. The complex was purified on a Sephadex LH-20 column (2 cm diam. × 30 cm) using acetone as the eluent. The major first band (brown) was collected and acetone was evaporated to obtain [{Ru(phen)$_2$}(μ-bb$_{12}$)-{Ru(phen)Cl$_2$}](PF$_6$)$_2$ as dark brown solid. The sample was transferred to a drying tube by dissolution in dichloromethane, which was removed *in vacuo* and the residue used for characterisation. **[{Ru(phen)$_2$}(μ-bb$_{12}$){Ru(phen)Cl$_2$}](PF$_6$)$_2$·0.5NH$_4$PF$_6$.** Anal. Calcd for $C_{70}H_{68}N_{10.5}Cl_2F_{15}P_{2.5}Ru_2$: C, 49.7%; H, 4.05%; N, 8.7%. Found: C, 49.6%; H, 3.67%; N, 8.3%. ^{1}H NMR (400 MHz, CD_3CN): δ 8.64 (d, J = 8.1 Hz, 4H); 8.54 (d, J = 8.3 Hz, 4H); 8.41–8.34 (m, 2H); 8.28–8.22 (m, 4H); 8.21–8.17 (m, 4H); 7.89–7.85 (m, 4H); 7.81–7.76 (m, 2H); 7.55 (dd, J = 7.8 Hz, 5.1 Hz, 4H); 7.48 (t, J = 5.0 Hz, 4H); 7.13–7.08 (m, 4H); 2.79–2.72 (m, 4H); 2.52 (s, 6H); 1.70–1.58 (m, 4H); 1.39–1.20 (m, 16H).

[{Ru(phen)$_2$}(μ-bb$_{16}$){Ru(phen)Cl$_2$}](PF$_6$)$_2$ and [{Ru(phen)$_2$}-(μ-bb$_{10}$){Ru(phen)Cl$_2$}](PF$_6$)$_2$ complexes were synthesised as reported above for [{Ru(phen)$_2$}(μ-bb$_{12}$){Ru(phen)Cl$_2$}](PF$_6$)$_2$. **[{Ru(phen)$_2$}(μ-bb$_{16}$){Ru(phen)Cl$_2$}](PF$_6$)$_2$·3CH$_2$Cl$_2$·C$_3$H$_6$O.** Anal. Calcd for $C_{80}H_{86}N_{10}Cl_8F_{12}OP_2Ru_2$: C, 48.5%; H, 4.38%; N, 7.1%. Found: C, 48.2%; H, 4.66%; N, 6.7%. ^{1}H NMR (400 MHz, CD_3CN): δ 8.64 (d, J = 8.1 Hz, 4H); 8.53 (d, J = 7.9 Hz, 4H); 8.42–8.34 (m, 2H); 8.27–8.22 (m, 4H); 8.21–8.16 (m, 4H); 7.89–7.85 (m, 4H); 7.79 (dd, J = 7.9 Hz, 5.0 Hz, 2H); 7.55 (dd, J = 8.0 Hz, 5.1 Hz, 4H); 7.48 (t, J = 5.2 Hz, 4H); 7.13–7.08 (m, 4H); 2.79–2.73 (m, 4H); 2.51 (s, 6H); 1.69–1.60 (m, 4H); 1.39–1.19(m, 24H). **[{Ru(phen)$_2$}(μ-bb$_{10}$){Ru(phen)Cl$_2$}](PF$_6$)$_2$·NH$_4$PF$_6$·2CH$_2$Cl$_2$.** Anal. Calcd for $C_{70}H_{70}N_{11}Cl_6F_{18}P_3Ru_2$: C, 43.9%; H, 3.68%; N, 8.1%. Found: C, 43.8%; H, 3.54%; N, 7.9%. ^{1}H NMR (400 MHz, CD_3CN): δ 8.65 (d, J = 7.9 Hz, 4H); 8.54 (d, J = 7.7 Hz, 4H); 8.42–8.34 (m, 2H); 8.28–8.16 (m, 8H); 7.90–7.84 (m, 4H); 7.82–7.75 (m, 2H); 7.55 (dd, J = 8.3 Hz, 5.3 Hz, 4H); 7.48 (t, J = 5.1 Hz, 4H); 7.14–7.07 (m, 4H); 2.80–2.72 (m, 4H); 2.51 (s, 6H); 1.72–1.58 (m, 4H); 1.42–1.21 (m, 12H).

The PF_6^- salts were converted to chloride salts with Amberlite IRA-402 (chloride form) anion-exchange resin. The PF_6^- salt of the complex was taken up in methanol (25 mL) and resin added and the mixture stirred at room temperature for 1–2 h until the solution was clear, the resin was then filtered and methanol was evaporated and the resultant solid dried in an oven at 70 °C for 16 h to obtain a dark brownish-orange solid of [{Ru(phen)$_2$}(μ-bb$_n$){Ru(phen)Cl$_2$}]Cl$_2$ (Rubb$_n$-Cl$_2$), typical yields were 60–65%, based on the synthetic starting material [Ru(phen)$_2$(bb$_n$)](PF$_6$)$_2$.

[{Ru(phen)$_2$}(μ-bb$_n$){Ru(phen)}(μ-bb$_n$){Ru(phen)$_2$}]Cl$_6$ (Rubb$_n$-tri). In a typical reaction, both the starting materials [{Ru-(phen)$_2$}(μ-bb$_{16}$){Ru(phen)Cl$_2$}](PF$_6$)$_2$ (125 mg, 0.075 mmol) and [Ru(phen)$_2$(bb$_{16}$)](PF$_6$)$_2$ (98 mg, 0.075 mmol) were dissolved in ethanol–water (1 : 1, 60 mL) and the mixture refluxed at 80 °C in the dark under a nitrogen atmosphere for 4 h. The colour of the reaction mixture slowly turned from dark brown to dark red during the course of the reaction. The reaction mixture was cooled to room temperature and the solvent was evaporated under reduced pressure to obtain a dark orange solid, the resulting solid was converted to chloride salt by stirring it in methanol using Amberlite IRA-402 (chloride form) anion-exchange resin for 1–2 h, after filtration of the resin, methanol was evaporated and the resultant chloride salt was dissolved in water (10 mL) and loaded onto an SP Sephadex C-25 cation exchange column (2 cm diam. × 25 cm), the column was washed with water and eluted with 0.6 M and then 0.8 M NaCl solutions to remove mono- and di-nuclear impurities. The desired trinuclear complex was eluted with 1 M NaCl solution containing 20% acetone. After removing the acetone, solid KPF_6 was added to the eluate and the complex was extracted into dichloromethane (2 × 30 mL). The organic layer was washed with water (20 mL), dried over anhydrous Na_2SO_4, and evaporated to dryness to obtain PF_6^- salt of the complex. The complex was further purified on Sephadex LH-20 (2 cm diam. × 30 cm) using acetone as the eluent. The major first orange band was collected and the acetone removed and the product crystallised using acetonitrile–toluene to obtain a bright red-orange solid of [{Ru(phen)$_2$}(μ-bb$_{16}$){Ru(phen)}-(μ-bb$_{16}$){Ru(phen)$_2$}](PF$_6$)$_6$. **[{Ru(phen)$_2$}(μ-bb$_{16}$){Ru(phen)}-(μ-bb$_{16}$){Ru(phen)$_2$}](PF$_6$)$_6$.** Anal. Calcd for $C_{136}H_{140}N_{18}F_{36}P_6Ru_3$: C, 51.0%; H, 4.41%; N, 7.9%. Found: C, 51.2%; H, 4.29%; N, 7.8%. ^{1}H NMR (400 MHz, CD_3CN): δ 8.67–8.60 (m, 5H); 8.57–8.49 (m, 5H); 8.43–8.34 (m, 8H); 8.29–8.17 (m, 18H); 7.88 (m, 5H); 7.82–7.76 (m, 5H); 7.59–7.51 (m, 8H); 7.48 (m, 5H); 7.14–7.07 (m, 5H); 2.82–2.72 (m, 8H); 2.57 (s, 3H); 2.51 (s, 6H); 2.47 (s, 3H); 1.72–1.59 (m, 8H); 1.39–1.17 (m, 48H). ^{13}C NMR (CD_3CN): δ 157.82, 157.76, 157.5, 155.7, 155.4, 153.57, 153.53, 153.48, 152.3, 152.1, 151.2, 148.8, 148.6, 137.55, 137.42, 131.9, 129.0, 128.9, 128.2, 126.86, 126.76, 125.7, 124.9, 35.6, 30.8, 30.4, 30.3, 30.2, 30.0, 29.9, 28.7, 21.4 and 21.0. TOF MS (ESI+): most abundant ion found for [M − 4PF$_6$]$^{4+}$, m/z 654.94. Calc. for Ru$_3$[C$_{136}$H$_{140}$N$_{18}$]-(PF$_6$)$_2^{4+}$, m/z 654.97; most abundant ion found for [M − 3PF$_6$]$^{3+}$, m/z 921.59. Calc. for Ru$_3$[C$_{136}$H$_{140}$N$_{18}$]-(PF$_6$)$_3^{3+}$, m/z 921.61; most abundant ion found for

$[M - 2PF_6]^{2+}$, *m/z* 1454.87. Calc. for $Ru_3[C_{136}H_{140}N_{18}](PF_6)_4^{2+}$, *m/z* 1454.90.

[{Ru(phen)$_2$}(μ-bb$_{12}$){Ru(phen)}(μ-bb$_{12}$){Ru(phen)$_2$}](PF$_6$)$_6$. Anal. Calcd for $C_{128}H_{124}N_{18}F_{36}P_6Ru_3$: C, 49.8%; H, 4.05%; N, 8.2%. Found: C, 50.1%; H, 3.82%; N, 8.2%. ^{1}H NMR (400 MHz, CD_3CN): *δ* 8.66–8.61 (m, 5H); 8.56–8.50 (m, 5H); 8.42–8.34 (m, 8H); 8.28–8.16 (m, 18H); 7.91–7.85 (m, 5H); 7.81–7.76 (m, 5H); 7.58–7.52 (m, 8H); 7.50–7.45 (m, 5H); 7.13–7.08 (m, 5H); 2.81–2.71 (m, 8H); 2.57 (s, 3H); 2.51 (s, 6H); 2.47 (s, 3H); 1.71–1.59 (m, 8H); 1.41–1.17 (m, 32H). ^{13}C NMR (CD_3CN): *δ* 157.8, 157.7, 157.5, 155.8, 154.9, 153.6, 153.5, 153.3, 152.3, 152.1, 151.2, 148.8, 148.5, 137.5, 137.4, 131.8, 129.0, 128.9, 128.4, 126.8, 126.7, 125.7, 124.9, 35.6, 30.9, 30.7, 30.4, 30.2, 30.1, 30.0, 29.8, 28.9, 21.1 and 20.8. TOF MS (ESI+): most abundant ion found for $[M - 4PF_6]^{4+}$, *m/z* 626.91. Calc. for $Ru_3[C_{128}H_{124}N_{18}](PF_6)_2^{4+}$, *m/z* 626.91; most abundant ion found for $[M - 3PF_6]^{3+}$, *m/z* 884.21. Calc. for $Ru_3[C_{128}H_{124}N_{18}](PF_6)_3^{3+}$, *m/z* 884.21; most abundant ion found for $[M - 2PF_6]^{2+}$, *m/z* 1399.78. calc. for $Ru_3[C_{128}H_{124}N_{18}](PF_6)_4^{2+}$, *m/z* 1399.30. **[{Ru(phen)$_2$}(μ-bb$_{10}$){Ru(phen)}(μ-bb$_{10}$){Ru(phen)$_2$}](PF$_6$)$_6$.** Anal. Calcd for $C_{124}H_{116}N_{18}F_{36}P_6Ru_3$: C, 49.1%; H, 3.86%; N, 8.3%. Found: C, 48.8%; H, 3.84%; N, 8.2%. ^{1}H NMR (400 MHz, CD_3CN): *δ* 8.68–8.61 (m, 5H); 8.57–8.50 (m, 5H); 8.42–8.33 (m, 8H); 8.28–8.16 (m, 18H); 7.90–7.85 (m, 5H); 7.81–7.76 (m, 5H); 7.57–7.52 (m, 8H); 7.51–7.45 (m, 5H); 7.13–7.08 (m, 5H); 2.82–2.70 (m, 8H); 2.56 (s, 3H); 2.51 (s, 6H); 2.47 (s, 3H); 1.73–1.58 (m, 8H); 1.43–1.22 (m, 24H). ^{13}C NMR (CD_3CN): *δ* 157.8, 157.74, 157.6, 155.6, 155.1, 153.56, 153.51, 153.3, 152.3, 152.1, 151.2, 148.8, 148.5, 137.54, 137.42, 131.8, 129.0, 128.9, 128.3, 126.8, 126.7, 125.7, 124.9, 35.6, 30.9, 30.8, 30.3, 30.2, 30.09, 30.01, 29.9, 29.6, 21.1 and 20.9. TOF MS (ESI+): most abundant ion found for $[M - 4PF_6]^{4+}$, *m/z* 612.89. Calc. for $Ru_3[C_{124}H_{116}N_{18}](PF_6)_2^{4+}$, *m/z* 612.89; most abundant ion found for $[M - 3PF_6]^{3+}$, *m/z* 865.52. Calc. for $Ru_3[C_{124}H_{116}N_{18}](PF_6)_3^{3+}$, *m/z* 865.50; most abundant ion found for $[M - 2PF_6]^{2+}$, *m/z* 1370.76. calc. for $Ru_3[C_{124}H_{116}N_{18}](PF_6)_4^{2+}$, *m/z* 1370.74.

The chloride salts were obtained by stirring the PF_6^- salts in methanol with Amberlite IRA-402 (chloride form) anion-exchange resin for 1–2 h until the solution was clear. The resin was removed by filtration, and the orange-red solution was evaporated and the solid dried in an oven at 70 °C for 16 h to obtain dark red solid of [{Ru(phen)$_2$}(μ-bb$_n$){Ru(phen)}(μ-bb$_n$){Ru(phen)$_2$}]Cl$_6$ (Rubb$_n$-tri), typical yields were 25–30%, based on the synthetic starting material [Ru(phen)$_2$(bb$_n$)](PF$_6$)$_2$.

[{Ru(phen)$_2$}(μ-bb$_n$){Ru(phen)}(μ-bb$_n$){Ru(phen)}(μ-bb$_n$){Ru(phen)$_2$}]Cl$_8$ (Rubb$_n$-tetra). In a typical reaction, [{Ru(phen)$_2$}(μ-bb$_{16}$){Ru(phen)Cl$_2$}](PF$_6$)$_2$ (95 mg, 0.057 mmol) was dissolved in ethanol–water (1 : 1, 50 mL) and bb$_{16}$ ligand (32 mg, 0.057 mmol) was added and the reaction mixture heated at reflux for 4 h in the dark under a nitrogen atmosphere. The colour of the reaction slowly turned from dark brown to dark red during the course of the reaction. The reaction mixture was cooled to room temperature and the solvent was evaporated under reduced pressure to obtain a dark orange-red solid, which was then converted to the chloride salt by stirring in methanol with Amberlite IRA-402 (chloride form) anion-exchange resin. After filtration of the resin, the methanol was evaporated to obtain the chloride salt which was dissolved in water (10 mL) and loaded onto an SP-Sephadex C-25 cation exchange column (2 cm diam. × 25 cm), the column washed with water and eluted with 0.6 M and then 0.8 M NaCl solutions to remove the impurities. The desired tetranuclear complex was eluted with a 1 M NaCl solution containing 30% acetone. After removing the acetone, solid KPF_6 was added to the eluate followed by extraction into DCM (2 × 20 mL). The organic layer was washed with water (20 mL), dried over anhydrous Na_2SO_4, and evaporated to dryness to obtain the PF_6^- salt of the complex. The complex was further purified using Sephadex LH-20 with acetone as the eluent. The major first orange band was collected, the acetone evaporated and the resultant solid crystallised from acetonitrile–toluene to yield a bright red-orange precipitate of [{Ru(phen)$_2$}(μ-bb$_{16}$){Ru(phen)}(μ-bb$_{16}$){Ru(phen)}(μ-bb$_{16}$){Ru(phen)$_2$}](PF$_6$)$_8$. **[{Ru(phen)$_2$}(μ-bb$_{16}$){Ru(phen)}(μ-bb$_{16}$){Ru(phen)}(μ-bb$_{16}$){Ru(phen)$_2$}](PF$_6$)$_8$.** Anal. Calcd for $C_{186}H_{198}N_{24}F_{48}P_8Ru_4$: C, 51.5%; H, 4.61%; N, 7.8%. Found: C, 51.4%; H, 4.42%; N, 7.8%. ^{1}H NMR (400 MHz, CD_3CN): *δ* 8.66–8.52 (m, 16H); 8.42–8.34 (m, 10H); 8.30–8.18 (m, 18H); 7.91–7.86 (m, 8H); 7.83–7.77 (m, 8H); 7.55 (m, 12H); 7.51–7.46 (m, 6H); 7.11 (m, 6H); 2.76 (m, 12H); 2.57 (s, 3H); 2.51 (s, 12H); 2.47 (s, 3H); 1.74–1.58 (m, 12H); 1.43–1.14 (m, 72H). ^{13}C NMR (CD_3CN): *δ* 157.8, 157.75, 156.9, 155.6, 153.55, 153.50, 153.46, 152.2, 152.1, 151.2, 148.8, 148.5, 137.5, 137.4, 131.85, 131.82, 128.9, 128.8, 128.7, 128.2, 126.8, 126.7, 125.6, 124.9, 35.6, 30.8, 30.7, 30.4, 30.3, 30.24, 30.19, 30.05, 30.01, 29.8, 29.7, 21.1 and 20.6. TOF MS (ESI+): most abundant ion found for $[M - 6PF_6]^{6+}$, *m/z* 577.36. Calc. for $Ru_4[C_{186}H_{198}N_{24}]$ $(PF_6)_2^{6+}$, *m/z* 577.33; most abundant ion found for $[M - 4PF_6]^{4+}$, *m/z* 938.55. Calc. for $Ru_4[C_{186}H_{198}N_{24}](PF_6)_4^{4+}$, *m/z* 938.48; most abundant ion found for $[M - 3PF_6]^{3+}$, *m/z* 1299.40. Calc. for $Ru_4[C_{186}H_{198}N_{24}](PF_6)_5^{3+}$, *m/z* 1299.63. **[{Ru(phen)$_2$}(μ-bb$_{12}$){Ru(phen)}(μ-bb$_{12}$){Ru(phen)}(μ-bb$_{12}$){Ru(phen)$_2$}](PF$_6$)$_8$.** Anal. Calcd for $C_{174}H_{174}N_{24}F_{48}P_8Ru_4$: C, 50.2%; H, 4.21%; N, 8.1%. Found: C, 50.2%; H, 4.35%; N, 8.0%. ^{1}H NMR (400 MHz, CD_3CN): *δ* 8.68–8.50 (m, 16H); 8.43–8.33 (m, 10H); 8.29–8.22 (m, 10H); 8.21–8.16 (m, 8H); 7.88 (m, 8H); 7.82–7.75 (m, 8H); 7.59–7.52 (m, 12H); 7.48 (m, 6H); 7.10 (m, 6H); 2.75 (m, 12H); 2.59 (s, 3H); 2.51 (s, 12H); 2.46 (s, 3H); 1.71–1.57 (m, 12H); 1.43–1.21 (m, 48H). ^{13}C NMR (CD_3CN): *δ* 157.79, 157.73, 155.6, 153.55, 153.52, 153.48, 152.29, 152.17, 151.2, 148.8, 148.5, 137.52, 137.41, 131.85, 131.81, 128.95, 128.91, 128.86, 128.1, 126.8, 126.7, 125.7, 124.9, 35.6, 30.8, 30.6, 30.35, 30.27, 30.23, 30.16, 30.04, 29.9, 29.8, 29.7, 21.1 and 20.5. TOF MS (ESI+): most abundant ion found for $[M - 6PF_6]^{6+}$, *m/z* 549.47. Calc. for $Ru_4[C_{174}H_{174}N_{24}](PF_6)_2^{6+}$, *m/z* 549.28; most abundant ion found for $[M - 5PF_6]^{5+}$, *m/z* 688.18. Calc. for $Ru_4[C_{174}H_{174}N_{24}](PF_6)_3^{5+}$, *m/z* 688.13; most abundant ion found for $[M - 4PF_6]^{4+}$, *m/z* 896.73. Calc. for $Ru_4[C_{174}H_{174}N_{24}](PF_6)_4^{4+}$, *m/z* 896.40. **[{Ru(phen)$_2$}(μ-bb$_{10}$){Ru(phen)}(μ-bb$_{10}$){Ru(phen)}(μ-bb$_{10}$){Ru(phen)$_2$}](PF$_6$)$_8$.** Anal. Calcd for $C_{168}H_{162}N_{24}F_{48}P_8Ru_4$: C, 49.4%; H, 4.00%; N, 8.2%. Found: C, 49.4%; H, 3.92%; N,

8.0%. ^{1}H NMR (400 MHz, CD_3CN): δ 8.68–8.51 (m, 16H); 8.41–8.33 (m, 10H); 8.28–8.22 (m, 10H); 8.21–8.15 (m, 8H); 7.87 (m, 8H); 7.81–7.76 (m, 8H); 7.54 (m, 12H); 7.50–7.46 (m, 6H); 7.12 (m, 6H); 2.78 (m, 12H); 2.56 (s, 3H); 2.51 (s, 12H); 2.45 (s, 3H); 1.73–1.56 (m, 12H); 1.45–1.22 (m, 36H). ^{13}C NMR (CD_3CN): δ 157.8, 157.7, 155.6, 153.56, 153.51, 153.46, 152.3, 152.2, 151.2, 148.8, 148.5, 137.5, 137.4, 131.8, 131.6, 128.94, 128.89, 128.82, 128.2, 126.8, 126.7, 125.6, 124.9, 35.6, 30.9, 30.6, 30.3, 30.2, 30.16, 30.08, 30.01, 29.9, 29.8, 29.7, 21.1 and 20.8. TOF MS (ESI+): most abundant ion found for $[M - 5PF_6]^{5+}$, m/z 671.40. Calc. for $Ru_4[C_{168}H_{162}N_{24}](PF_6)_3^{5+}$, m/z 671.29; most abundant ion found for $[M - 4PF_6]^{4+}$, m/z 875.77. Calc. for $Ru_4[C_{168}H_{162}N_{24}](PF_6)_4^{4+}$, m/z 875.36; most abundant ion found for $[M - 3PF_6]^{3+}$, m/z 1215.32. Calc. for $Ru_4[C_{168}H_{162}N_{24}](PF_6)_5^{3+}$, m/z 1215.47.

The chloride salts were obtained by stirring the PF_6^- salts in methanol with Amberlite IRA-402 (chloride form) anion-exchange resin. The resin was removed by filtration, and the orange-red solution was evaporated and dried in oven at 70 °C for 16 h to obtain dark red $[\{Ru(phen)_2\}(\mu\text{-}bb_n)\{Ru(phen)\}(\mu\text{-}bb_n)\{Ru(phen)\}(\mu\text{-}bb_n)\{Ru(phen)_2\}]Cl_8$ ($Rubb_{16}$-tetra), typical yields were 20–25%, based on the synthetic starting material $[\{Ru(phen)_2\}(\mu\text{-}bb_n)\{Ru(phen)Cl_2\}](PF_6)_2$.

$[\{Ru(\mu\text{-}bb_n)_3\}\{Ru(phen)_2\}_3]Cl_8$ ($Rubb_n$-tetra-nl). In a typical reaction, a mixture of $[Ru(phen)_2(bb_{16})](PF_6)_2$ (229 mg, 0.174 mmol) and *cis*-$[Ru(DMSO)_4Cl_2]$ (28 mg, 0.057 mmol) was heated to reflux in ethanol–water (1 : 1, 20 mL) for 5–6 h under the nitrogen atmosphere. The reaction mixture was cooled to room temperature and the solvent evaporated to obtain an orange solid which was converted to the chloride salt by stirring in methanol with Amberlite IRA-402 (chloride form) anion-exchange resin. After filtration of the resin and removal of methanol, the solid was dissolved in water (10 mL) and loaded onto an SP-Sephadex C-25 cation exchange column (2 cm diam. × 25 cm), eluted with water and then with 0.6 M and then 0.8 M NaCl solutions to remove the impurities. The desired non-linear tetranuclear complex was eluted with a 1 M NaCl solution containing 30% acetone. After removing the acetone, solid KPF_6 was added to the eluate followed by extraction into DCM (2 × 20 mL). The organic layer was washed with water (20 mL), dried over anhydrous Na_2SO_4, and evaporated to dryness to obtain the PF_6^- salt of the complex. The complex was further purified using Sephadex LH-20 with acetone as the eluent, the major first orange band was collected and the acetone evaporated to yield a bright red-orange solid of $[\{Ru(\mu\text{-}bb_{16})_3\}\{Ru(phen)_2\}_3](PF_6)_8$. **$[\{Ru(\mu\text{-}bb_{16})_3\}\{Ru(phen)_2\}_3](PF_6)_8$.** Anal. Calcd for $C_{186}H_{198}N_{24}F_{48}P_8Ru_4$: C, 51.5%; H, 4.61%; N, 7.8%. Found: C, 51.2%; H, 4.66%; N, 7.7%. ^{1}H NMR (400 MHz, CD_3CN): δ 8.67–8.62 (m, 8H); 8.57–8.51 (m, 8H); 8.44–8.36 (m, 10H); 8.26–8.22 (m, 10H); 8.21–8.18 (m, 8H); 7.92–7.84 (m, 8H); 7.82–7.76 (m, 8H); 7.58–7.52 (m, 12H); 7.49–7.45 (m, 6H); 7.14–7.07 (m, 6H); 2.74 (m, 12H); 2.64 (s, 3H); 2.54 (s, 12H); 2.44 (s, 3H); 1.73–1.57 (m, 12H); 1.44–1.16 (m, 72H). ^{13}C NMR (CD_3CN): δ 157.8, 157.7, 156.9, 156.5, 156.3, 155.7, 154.8, 153.7, 153.57, 153.53, 153.49, 152.3, 152.2, 151.2, 148.8, 148.6, 137.5, 137.4, 131.8, 129.0, 128.9, 128.8, 128.2, 126.8, 126.7, 125.7, 124.9, 35.6, 30.9, 30.6, 30.48, 30.40, 30.3, 30.2, 30.1, 30.04, 29.96, 29.91, 28.5, 21.1 and 20.7. TOF MS (ESI+): most abundant ion found for $[M - 8PF_6]^{8+}$, m/z 396.77. Calc. for $Ru_4[C_{186}H_{198}N_{24}]^{8+}$, m/z 396.76; most abundant ion found for $[M - 7PF_6]^{7+}$, m/z 474.10. Calc. for $Ru_4[C_{186}H_{198}N_{24}](PF_6)_1^{7+}$, m/z 474.14; most abundant ion found for $[M - 5PF_6]^{5+}$, m/z 721.90. Calc. for $Ru_4[C_{186}H_{198}N_{24}](PF_6)_3^{5+}$, m/z 721.79. **$[\{Ru(\mu\text{-}bb_{12})_3\}\{Ru(phen)_2\}_3](PF_6)_8\cdot 4H_2O$.** Anal. Calcd for $C_{174}H_{182}N_{24}F_{48}O_4P_8Ru_4$: C, 49.3%; H, 4.33%; N, 7.9%. Found: C, 48.9%; H, 4.36%; N, 7.6%. ^{1}H NMR (400 MHz, CD_3CN): δ 8.68–8.63 (m, 8H); 8.56–8.52 (m, 8H); 8.42–8.34 (m, 10H); 8.28–8.22 (m, 10H); 8.21–8.17 (m, 8H); 7.90–7.86 (m, 8H); 7.84–7.78 (m, 8H); 7.57–7.52 (m, 12H); 7.50–7.46 (m, 6H); 7.13–7.08 (m, 6H); 2.77 (m, 12H); 2.62 (s, 3H); 2.52 (s, 12H); 2.45 (s, 3H); 1.71–1.56 (m, 12H); 1.41–1.14 (m, 48H). ^{13}C NMR (CD_3CN): δ 157.8, 157.7, 156.8, 156.2, 156.0, 155.6, 154.5, 153.9, 153.6, 153.4, 152.3, 152.2, 151.2, 148.8, 148.6, 137.5, 137.4, 131.8, 129.0, 128.95, 128.89, 128.2, 126.8, 126.7, 125.7, 124.9, 35.6, 30.9, 30.7, 30.4, 30.3, 30.2, 30.1, 30.06, 30.02, 29.9, 29.3, 28.3, 21.2 and 21.1. TOF MS (ESI+): most abundant ion found for $[M - 8PF_6]^{8+}$, m/z 375.75. Calc. for $Ru_4[C_{174}H_{174}N_{24}]^{8+}$, m/z 375.71; most abundant ion found for $[M - 7PF_6]^{7+}$, m/z 450.00. Calc. for $Ru_4[C_{174}H_{174}N_{24}](PF_6)_1^{7+}$, m/z 450.10; most abundant ion found for $[M - 6PF_6]^{6+}$, m/z 549.16. Calc. for $Ru_4[C_{174}H_{174}N_{24}](PF_6)_2^{6+}$, m/z 549.28; most abundant ion found for $[M - 5PF_6]^{5+}$, m/z 688.18. Calc. for $Ru_4[C_{174}H_{174}N_{24}](PF_6)_3^{5+}$, m/z 688.13. **$[\{Ru(\mu\text{-}bb_{10})_3\}\{Ru(phen)_2\}_3](PF_6)_8\cdot 4H_2O$.** Anal. Calcd for $C_{168}H_{170}N_{24}F_{48}O_4P_8Ru_4$: C, 48.6%; H, 4.13%; N, 8.1%. Found: C, 48.5%; H, 4.37%; N, 7.7%. ^{1}H NMR (400 MHz, CD_3CN): δ 8.69–8.62 (m, 8H); 8.57–8.52 (m, 8H); 8.44–8.31 (m, 10H); 8.29–8.22 (m, 10H); 8.21–8.16 (m, 8H); 7.91–7.85 (m, 8H); 7.82–7.76 (m, 8H); 7.58–7.52 (m, 12H); 7.51–7.46 (m, 6H); 7.13–7.07 (m, 6H); 2.76 (m, 12H); 2.60 (s, 3H); 2.54 (s, 12H); 2.44 (s, 3H); 1.72–1.60 (m, 12H); 1.42–1.20 (m, 36H). ^{13}C NMR (CD_3CN): δ 157.8, 157.7, 157.0, 156.9, 156.4, 155.9, 155.6, 155.3, 153.57, 153.52, 153.4, 153.3, 152.3, 152.1, 151.2, 150.8, 148.8, 148.5, 137.5, 137.4, 131.8, 128.96, 128.90, 128.2, 126.8, 126.7, 125.7, 124.9, 35.6, 30.96, 30.91, 30.6, 30.2, 30.08, 30.01, 29.8, 29.3, 28.3, 21.2 and 20.9. TOF MS (ESI+): most abundant ion found for $[M - 5PF_6]^{5+}$, m/z 671.36. Calc. for $Ru_4[C_{168}H_{162}N_{24}](PF_6)_3^{5+}$, m/z 671.29; most abundant ion found for $[M - 4PF_6]^{4+}$, m/z 875.45. Calc. for $Ru_4[C_{168}H_{162}N_{24}](PF_6)_4^{4+}$, m/z 875.36; most abundant ion found for $[M - 3PF_6]^{3+}$, m/z 1215.60. Calc. for $Ru_4[C_{168}H_{162}N_{24}](PF_6)_5^{3+}$, m/z 1215.47; most abundant ion found for $[M - 2PF_6]^{2+}$, m/z 1895.85. Calc. for $Ru_4[C_{168}H_{162}N_{24}](PF_6)_6^{2+}$, m/z 1895.69.

The chloride salts were obtained by stirring the PF_6^- salts in methanol with Amberlite IRA-402 (chloride form) anion-exchange resin. The resin was removed by filtration, and the orange-red solution was evaporated and dried in oven at 70 °C for 16 h to obtain dark red $[\{Ru(\mu\text{-}bb_n)_3\}\{Ru(phen)_2\}_3]Cl_8$ ($Rubb_n$-tetra-nl), typical yields were 25–35%, based on the synthetic starting material $[Ru(DMSO)_4Cl_2]$.

Acknowledgements

We gratefully thank Ms Anitha Jeyasingham from the Mass Spectrometry Facility at the Research School of Chemistry, Australian National University, for the mass spectral data.

References

1 H. W. Boucher, G. H. Talbot, J. S. Bradley, J. E. Edwards Jr., D. Gilbert, L. B. Rice, M. Scheld, B. Spellberg and J. Bartlett, IDSA Report on Development Pipeline, 2009, **48**, 1.
2 E. Wong and C. M. Giandomenico, *Chem. Rev.*, 1999, **99**, 2451.
3 N. Farrell, in *Platinum-Based Drugs in Cancer Therapy*, ed. L. R. Kelland and N. Farrell, Humana Press, Totowa, NJ, 2000, pp. 321–338.
4 N. J. Wheate and J. G. Collins, *Coord. Chem. Rev.*, 2003, **241**, 133.
5 A. D. Richards, A. Rodger, M. J. Hannon and A. Bolhuis, *Intl. J. Antimicrobial Agents*, 2009, **33**, 469.
6 A. Anthonysamy, S. Balasubramanian, V. Shanmugaiah and N. Mathivanan, *Dalton Trans.*, 2008, 2136.
7 K. A. Kumar, K. L. Reddy, S. Vidhisha and S. Satyanarayana, *Appl. Organomet. Chem.*, 2009, **23**, 409.
8 B. Biersack, R. Diestel, C. Jagusch, F. Sasse and R. Schobert, *J. Inorg. Biochem.*, 2009, **103**, 72.
9 A. Bolhuis, L. Hand, J. E. Marshall, A. D. Richards, A. Rodger and J. Aldrich-Wright, *Eur. J. Pharm. Sci.*, 2011, **42**, 313.
10 P. L. Lam, G.-L. Lu, K.-M. Hon, K.-W. Lee, C.-L. Ho, X. Wang, J. C.-O. Tang, K.-H. Lam, R. S.-M. Wong, S. H.-L. Kok, Z.-X. Bian, H. Li, K. K.-H. Li, R. Gambari, C.-H. Chui and W.-Y. Wong, *Dalton Trans.*, 2014, **43**, 3949.
11 F. P. Dwyer, E. C. Gyarfas, W. P. Rogers and J. H. Koch, *Nature*, 1952, **170**, 190.
12 F. P. Dwyer, I. K. Reid, A. Shulman, G. M. Laycock and S. Dixson, *Aust. J. Exp. Biol. Med. Sci.*, 1969, **47**, 203.
13 F. Li, Y. Mulyana, M. Feterl, J. Warner, J. G. Collins and F. R. Keene, *Dalton Trans.*, 2011, **40**, 5032.
14 F. Li, M. Feterl, Y. Mulyana, J. M. Warner, J. G. Collins and F. R. Keene, *J. Antimicrob. Chemother.*, 2012, **67**, 2686.
15 M. Pandrala, F. Li, M. Feterl, Y. Mulyana, J. M. Warner, L. Wallace, F. R. Keene and J. G. Collins, *Dalton Trans.*, 2013, **42**, 4686.
16 F. Li, E. J. Harry, A. L. Bottomley, M. D. Edstein, G. W. Birrell, C. E. Woodward, F. R. Keene and J. G. Collins, *Chem. Sci.*, 2014, **5**, 685.
17 M. Pandrala, F. Li, L. Wallace, P. J. Steel, B. Moore II, J. Autschbach, J. G. Collins and F. R. Keene, *Aust. J. Chem.*, 2013, **66**, 1065.
18 M. J. Hannon, *Pure Appl. Chem.*, 2007, **79**, 2243.
19 B. M. Zeglis, V. C. Pierre and J. K. Barton, *Chem. Commun.*, 2007, 4565.
20 F. R. Keene, J. A. Smith and J. G. Collins, *Coord. Chem. Rev.*, 2009, **253**, 2021.
21 M. R. Gill and J. A. Thomas, *Chem. Soc. Rev.*, 2012, **41**, 3179.
22 P. Lincoln and B. Nordén, *Chem. Commun.*, 1996, 2145.
23 J. Malina, M. J. Hannon and V. Brabec, *Chem. – Eur. J.*, 2008, **14**, 10408.
24 M. R. Gill, J. Garcia-Lara, S. J. Foster, C. Smythe, G. Battaglia and J. A. Thomas, *Nat. Chem.*, 2009, **1**, 662.
25 U. McDonnell, J. M. C. A. Kerchoffs, R. P. M. Castineiras, M. R. Hicks, A. C. G. Hotze, M. J. Hannon and A. Rodger, *Dalton Trans.*, 2008, 667.
26 X.-L. Zhao, Z.-S. Li, Z.-B. Zheng, A.-G. Zhang and K.-Z. Wang, *Dalton Trans.*, 2013, **42**, 5764.
27 D. R. Boer, L. Wu, P. Lincoln and M. Coll, *Angew. Chem., Int. Ed.*, 2014, **53**, 1949.
28 A. K. Renfrew, *Metallomics*, 2014, **6**, 1324.
29 B. Therrien, G. Süss-Fink, P. Govindaswamy, A. K. Renfrew and P. J. Dyson, *Angew. Chem., Int. Ed.*, 2008, **47**, 3773.
30 G. Süss-Fink, *Dalton Trans.*, 2010, **39**, 1673.
31 X. Li, X.-J. Li, Z.-Y. Wu and C.-W. Yan, *New J. Chem.*, 2012, **36**, 2472.
32 W. Luo, X.-G. Meng, G.-Z. Chen and Z.-P. Ji, *Inorg. Chim. Acta*, 2009, **362**, 551.
33 Y. Mulyana, D. K. Weber, P. D. Buck, C. A. Motti, J. G. Collins and F. R. Keene, *Dalton Trans.*, 2011, **40**, 1510.
34 N. C. Fletcher, M. Nieuwenhuyzen and S. Rainey, *J. Chem. Soc., Dalton Trans.*, 2001, 2641.
35 P. M. van Vliet, J. G. Haasnoot and J. Reedijk, *Inorg. Chem.*, 1994, **33**, 1934.
36 E. A. Seddon and K. R. Seddon, *The Chemistry of Ruthenium*, Elsevier, Amsterdam, 1984.
37 M. G. Sauaia, E. Tfouni, R. H. de Almeida Santos, M. T. do Prado Gambardella, M. P. F. M. Del Lama, L. F. Guimaraes and R. S. da Silva, *Inorg. Chem. Commun.*, 2003, **6**, 864.
38 A. Juris, V. Balzani, F. Barigelletti, S. Campagna, P. Belser and A. Von Zelewsky, *Coord. Chem. Rev.*, 1988, **84**, 85.
39 Y. Kawanishi, N. Kitamura and S. Tazuke, *Inorg. Chem.*, 1989, **28**, 2968.
40 A. B. P. Lever, *Inorg. Chem.*, 1990, **29**, 1271.
41 A. Macatangay, G. Y. Zheng, D. P. Rillema, D. C. Jackman and J. W. Merkert, *Inorg. Chem.*, 1996, **35**, 6823.
42 A. Bouskila, B. Drahi, E. Amouyal, I. Sasaki and A. Gaudemer, *J. Photochem. Photobiol., A*, 2004, **163**, 381.
43 M. Furue, N. Kuroda and S. Nozakura, *Chem. Lett.*, 1986, 1209.
44 M. Cavazzini, S. Quici, C. Scalera, F. Puntoriero, G. La Ganga and S. Campagna, *Inorg. Chem.*, 2009, **48**, 8578.
45 M. Staffilani, E. Höss, U. Giesen, E. Schneider, F. Hartl, H.-P. Josel and L. De Cola, *Inorg. Chem.*, 2003, **42**, 7789.
46 F. Li, M. Feterl, J. M. Warner, F. R. Keene and J. G. Collins, *J. Antimicrob. Chemother.*, 2013, **68**, 2825.
47 F. Li, *PhD thesis*, *Inert dinuclear polypyridylruthenium(II) complexes as antimicrobial agents*, University of New South Wales, Australia, 2013.

48 J. L. Morgan, C. B. Spillane, J. A. Smith, P. D. Buck, J. G. Collins and F. R. Keene, *Dalton Trans.*, 2007, 4333.
49 X. Hua and A. V. Zelewsky, *Inorg. Chem.*, 1995, **34**, 5791.
50 T. Tagano, *Inorg. Chim. Acta*, 1992, **195**, 221.
51 I. P. Evans, A. Spencer and G. Wilkinson, *J. Chem. Soc., Dalton Trans.*, 1973, 204.
52 Clinical and Laboratory Standards Institute, *Performance Standards for Antimicrobial Susceptibility Testing: Nineteenth Informational Supplement M100-S19*, CLSI, Wayne, PA, USA, 2009.
53 M. Motyl, K. Dorso, J. Barrett and R. Giacobbe, *Current Protocols in Pharmacology*, John Wiley & Sons, New York, 2005, 13A.3.1–13A.3.22.
54 D. Bao, B. Millare, W. Xia, B. G. Steyer, A. A. Gerasimenko, A. Ferreira, A. Contreras and V. I. Vullev, *J. Phys. Chem. A*, 2009, **113**, 1259.